Adsorption (2013) 19:501–508
DOI 10.1007/s10450-013-9472-0

Effects of carbon nanotube functionalization on the agglomeration and sintering of supported Pd nanoparticles

Róbert Puskás · Ákos Kukovecz · Zoltán Kónya

Received: 30 November 2012 / Accepted: 8 January 2013 / Published online: 18 January 2013

Abstract The size of carbon nanotube supported Pd and PdO nanoparticles was investigated on oxidatively functionalized multiwall carbon nanotubes. All samples were characterized by transmission electron microscopy, X-ray diffractometry, X-ray photoelectron spectroscopy and Raman spectroscopy. The average particle diameter calculated from TEM image analysis was found to be inversely proportional with the duration of the oxidation in nitric acid. Crystallite sizes determined from XRD patterns confirmed this general tendency.

Keywords Carbon nanotube · Functionalization · Palladium nanoparticle · Size dependence

1 Introduction

The field of catalysis has attracted a great amount of interest from researchers in the last century and remained a vigorously investigated area ever since. There are many aspects of catalysis which are still subjects of debates, thus the need for additional research has not diminished over time. One such aspect is the field of catalyst preparation, more precisely, the reproducible synthesis of supported metal catalysts which can be made in several different ways. Even laboratories working on the same "metal@support" composition regularly face difficulties in reproducing each other's results because of the effects of fine preparation detail differences on the performance of the end product.

Many types of supports exist and they are mostly based on various silica, alumina, titania, and carbon materials (Dalai and Davis 2008; Antolini 2012; Horvath et al. 2009). These all feature considerably different chemical and physical properties and therefore, even by dispersing the same active metallic phase over each one it is typical to obtain supported metal catalysts of different performances. In order to properly investigate the effects of the support on the catalyst system behavior, it is necessary to minimize any deliberately introduced differences between supports and make sure that comparisons are made using supports in exactly the same physico-chemical conditions.

Carbon nanotubes (CNTs) are good examples of catalyst support materials suffering from contradictory literature reports, therefore, they make good candidates for a detailed analysis of the pretreatment conditions on the properties of the final catalyst material. CNTs are widely discussed in scientific literature as support materials because of the great morphological and structural variety they offer (Serp et al. 2003). Single walled, double walled, few walled and multiwalled CNTs (Wu et al. 2012; Vermisoglou et al. 2011; Wu et al. 2011; Tang et al. 2010; Zhang 2012; Puskas et al. 2012) can easily be synthesized nowadays by a variety of techniques such as chemical vapor deposition (Puskas et al. 2012; Park et al. 2003; Yabe et al. 2004; Dikonimos Makrisa et al. 2004; Corrias et al. 2003; Hernadi et al. 2003), electric arc discharge (Antisari et al. 2003), laser vaporization (Lebedkin et al. 2002) and flame pyrolysis method (Height

R. Puskás · Á. Kukovecz · Z. Kónya
Department of Applied and Environmental Chemistry, University of Szeged, Rerrich Béla tér 1, Szeged 6720, Hungary

Á. Kukovecz (✉)
MTA-SZTE "Lendület" Porous Nanocomposites Research Group, Rerrich ter 1, Szeged 6720, Hungary
e-mail: kakos@chem.u-szeged.hu

Z. Kónya
MTA-SZTE Reaction Kinetics and Surface Chemistry Research Group, Rerrich ter 1, Szeged 6720, Hungary

et al. 2004). By using solvent or mechanical grinding based functionalization techniques, functional groups can be introduced onto the surface of CNTs (Silva et al. 2012; Konya et al. 2002), which allow further tuning of the support for more specific catalytic needs.

There are numerous methods to introduce metal nanoparticles onto the surface of a support like impregnation (Komiyama 1985), co-precipitation (Geus and van Dillen 1999), deposition–precipitation (Che and Bennett 1989), ion-exchange (Sachtler 1997), usage of preformed metal clusters (Gates 1995), deposition of preformed colloids (Che and Bennett 1989) or ligated nanoparticles (Bayram et al. 2010). These techniques are all regularly utilized for creating metal@CNT type supported heterogeneous catalysts as well. The performance differences of the obtained materials are typically attributed to e.g. different metal loadings, different CNT diameter or length, different functional group introduced onto the nanotube etc. Some application examples of metal nanoparticle loaded carbon nanotube catalysts include ethanol reforming (Seelam et al. 2010), cyclohexene hydrogenation (Sapi et al. 2009), Fischer–Tropsch synthesis (Xiong et al. 2011) and propene hydrogenation (Halonen et al. 2010).

In this contribution, we investigate the effect of the duration of the oxidation functionalization of multiwall carbon nanotubes (MWCNTs) on the average diameter of palladium nanoparticles created by impregnation and subsequent reduction in hydrogen flow. We demonstrate that even when all other parameters are kept constant, this single variable can affect the resulting Pd@MWCNT material considerably. The reported findings are believed to be a new addition to the knowledge pool of metal nanoparticle decoration of carbon nanotubes (Georgakilas et al. 2007).

2 Experimental

2.1 Sample preparation

Multiwalled carbon nanotubes (MWCNT) and functionalized multiwalled carbon nanotubes (FMWCNT) were used as support materials for all experiments. MWCNTs were prepared in our laboratory by the catalytic chemical vapor deposition (CCVD) method described elsewhere (Kukovecz et al. 2000). All FMWCNTs were prepared by thermally assisted oxidation of MWCNTs by refluxing a fixed amount of nanotubes (1 g) in a concentrated solution of HNO_3 (250 cm^3) for 4, 8, 12 and 16 h. Functionalization was followed by washing to pH 7 with distilled water and drying in air at 80 °C overnight. Noble metal nanoparticles were impregnated onto the dried nanotubes by the wet impregnation method using a toluene solution of Pd-acetate. 50 cm^3 of toluene and 11 mg of Pd-acetate was used for the impregnation of 100 mg CNT support. The mixture was sonicated for 15 min in a 80 W ultrasound bath, then stirred for 24 h at room temperature, then centrifuged at 3000 rpm and dried in air at 80 °C overnight. The as-prepared samples were finally annealed in air for 2 h at 185 °C and 1 h at 380 °C to form the impregnated intermediate for further processing.

All intermediate materials were divided into three parts: one was kept as reference, while the second and third were subjected to a second calcination process at 380 °C in air for 3 h or in N_2–H_2 (10:1, 330 cm^3/min) gas flow for 3 h, respectively. This procedure resulted in carbon nanotube supported PdO and Pd nanoparticles. The impregnated CNTs will be denoted by using the "PdO-"and "Pd-"prefixes for air calcined and hydrogen reduced samples respectively, whereas the "-380" suffix will denote the second calcination process when applicable.

2.2 Sample characterization

Transmission electron microscopy (TEM) was performed using a FEI Tecnai G^2 20 X-TWIN microscope with the tungsten cathode operated at 200 kV. Powder X-ray diffraction (XRD) patterns were obtained using a Rigaku Miniflex II instrument using Cu Kα radiation. The average diameter of the palladium nanoparticles was calculated both from XRD patterns using the Scherrer equation and by TEM image analysis. X-ray photoelectron spectroscopy (XPS) measurements were conducted using a SPECS instrument equipped with a PHOIBOS 150 MCD 9 hemispherical analyzer. The analyzer was operated in FAT mode with 20 eV pass energy. The Al Kα anode ($h\nu = 1486.6$ eV) was operated at 210 W (14 kV, 15 mA). Spectra were collected using 25 meV steps and 100 ms collection time for each data point per channel. Five consecutive measurements were summed up to obtain a spectrum. Raman spectra were measured using 785 nm laser excitation on an ocean optics QE65000 spectrometer.

3 Results and discussion

3.1 X-ray diffraction

The formation of PdO and Pd crystallites was confirmed by XRD. Figure 1 depicts the characteristic diffraction patterns of reference PdO containing (1a) as well as 380 °C calcined PdO containing (1b) and reduced Pd containing (1c) functionalized multiwall carbon nanotubes. Peaks corresponding to the crystal lattice planes of PdO and Pd with Miller indexes of (101) (112) (103) (211) and (111) (200) (220) (311) at *d*-spacing values of 2.63, 1.66, 1.53,

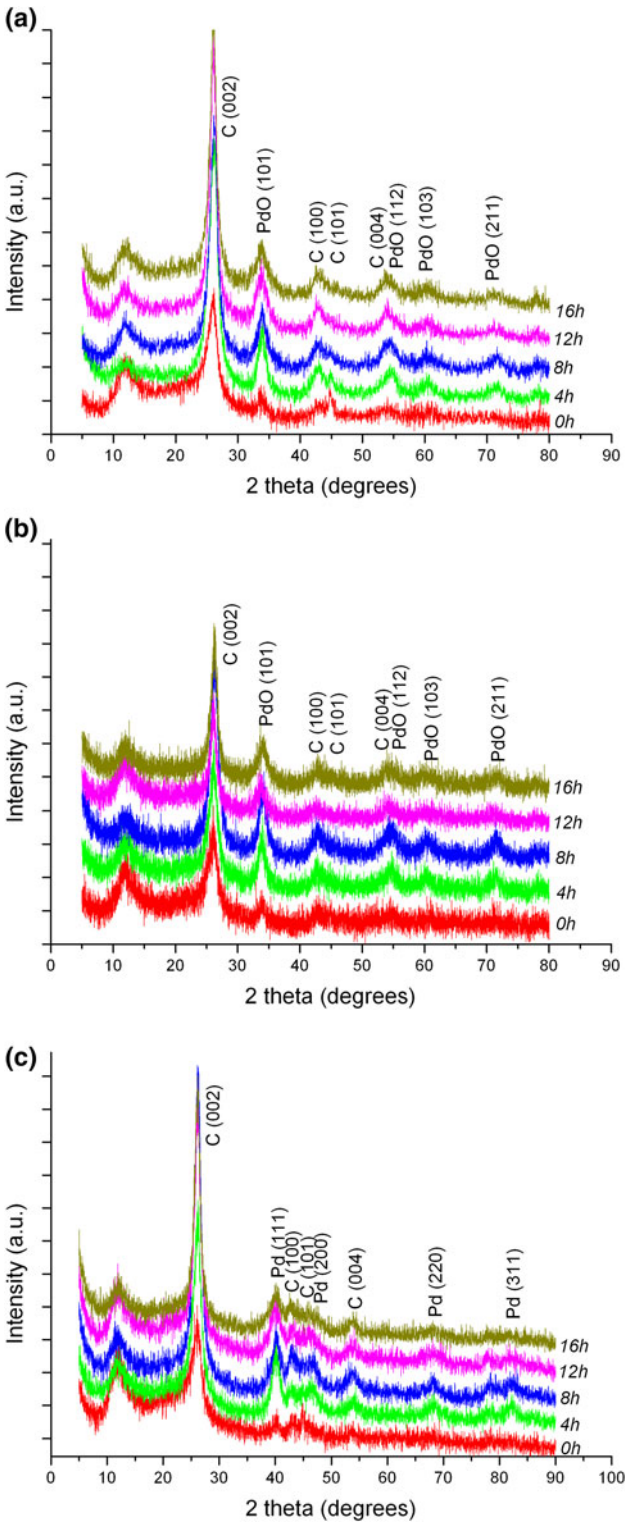

Fig. 1 XRD patterns of all prepared samples: PdO-FMWCNT series in part (**a**), PdO-FMWCNT-380 series in part (**b**) and Pd-FMWCNT-380 series in part (**c**)

1.31 and 2.24, 1.93, 1.37, 1.17 Å, respectively are observable. The crystallite sizes were calculated from the full width at half maximum (FWHM) values of the PdO (101) and Pd (111) peaks. Particle diameter data obtained by this Scherrer method are tabulated in Table 1.

Table 1 Nanoparticle diameters as calculated from FWHM values of the corresponding XRD peaks using the Scherrer equation

	0 h	4 h	8 h	12 h	16 h
PdO-FMWCNT	5.9	5.6	4.9	3.7	3.2
PdO-FMWCNT-380	7.2	6.4	5.4	4.8	4.2
Pd-FMWCNT-380	7.2	4.6	3.9	3.2	3.0

All data are given in nanometers

Gallagher and Gross have studied the thermal decomposition of palladium acetate in detail (Gallagher and Gross 1986) and concluded that the compound decomposes between 200 and 300 °C at atmospheric pressure in air. However, the decomposition is exothermic and therefore, sublimation of palladium acetate at local hotspots induced by thermal runaway events cannot be excluded in general. Under our specific experimental conditions the decomposition of palladium acetate can be considered complete and the role of volatilization is minor at the most.

It is interesting to note that the duration of the oxidative functionalization of the nanotube support has affected the size of the subsequently formed PdO and Pd nanoparticles. Crystallites synthesized on unfunctionalized nanotubes were the largest and those prepared on FMWCNTs treated for 16 h were the smallest. All others fell between these two extremes and showed an inverse correlation between nanoparticle diameter and functionalization duration. The PdO-FMWCNT-380 sample series exhibited the largest diameters by comparison to the other series which is probably the result of sintering during the secondary annealing process. Pd nanoparticles formed in the Pd-FMWCNT-380 series were generally the smallest, because the original, unsintered PdO crystals become more compact with the removal of the oxygen atoms from the crystal structure. It is also noticeable that samples subjected to the secondary annealing step exhibited the largest diameters on unfunctionalized supports, whereas Pd crystallites formed on the other samples were significantly smaller. This could indicate that surface inhomogeneities may possess different sintering inhibition ability towards oxide and metallic nanoparticles.

3.2 Transmission electron microscopy

TEM images of carbon nanotube supported nanoparticles are presented in Fig. 2. The apparent morphology of the carbon nanotubes remained intact during the processing. The nanoparticles are evenly dispersed on the surface of nanotubes and non-supported standalone particles are not observable. Nanoparticle diameter data obtained by TEM image analysis are summarized in Table 2.

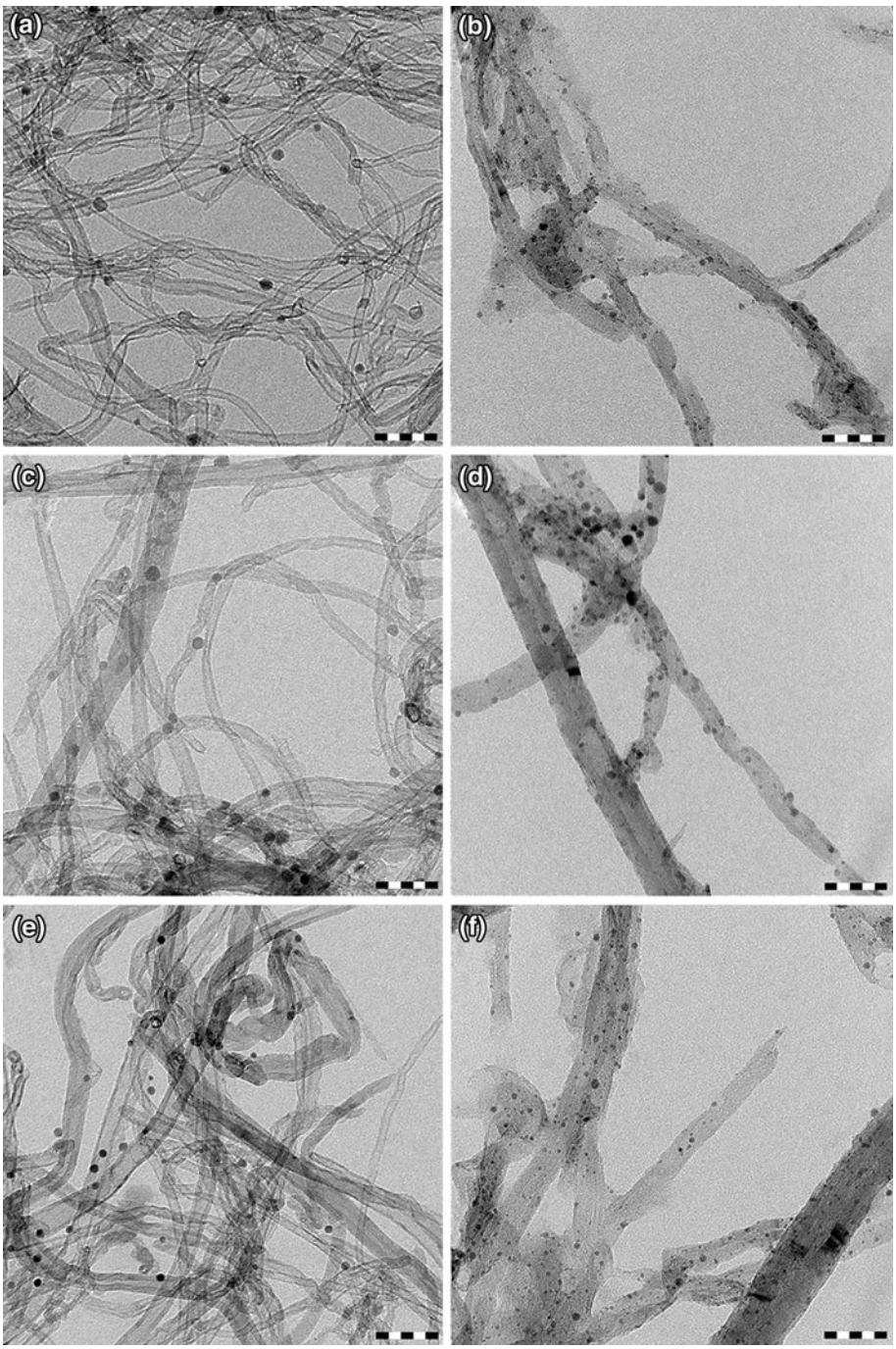

Fig. 2 Characteristic TEM micrographs of **a** 0 h PdO-FMWCNT, **b** 16 h PdO-FMWCNT, **c** 0 h PdO-FMWCNT-380, **d** 16 h PdO-FMWCNT-380, **e** 0 h Pd-FMWCNT-380 and **f** 16 h Pd-FMWCNT-380 samples. The *scale bar* marks 50 nm in each image

The TEM-derived average particle diameter data confirm the results of the XRD study insofar as the average nanoparticle diameter is inversely proportional with the duration of the functionalization reaction. Earlier Liu et al. have observed a reduction in the average diameter of Ni nanoparticles from 65 to 58 nm when synthesized on CNTs refluxed in 4 M nitric acid for 0.5 h (Liu et al. 2005). Another interesting phenomenon is observed when the diameters in different sample series are compared. Despite the second 3 h annealing process suffered by the samples of the PdO-FMWCNT-380 series, the measured average diameter of the PdO nanoparticles was lower on these samples then on those of the PdO-FMWCNT series. This phenomenon could originate from the fact that particles seen in TEM micrographs are in many cases built up from smaller, usually visually indistinguishable crystallites. These can sinter at high temperatures, resulting in denser particles made of smaller crystallites after annealing, The sintering is accompanied by the loss of inter-crystalline voids characteristic of the particle agglomerates before heat treatment.

Table 2 Average nanoparticle diameters obtained by TEM micrograph image analysis

	0 h	4 h	8 h	12 h	16 h
PdO-FMWCNT	8.0	7.5	6.9	5.2	5.6
PdO-FMWCNT-380	8.5	6.8	5.7	4.8	4.3
Pd-FMWCNT-380	6.4	5.1	4.0	3.4	3.1

All data are given in nanometers

This hypothesis is supported by the comparison of particle diameters obtained by XRD and TEM. Figure 4a reveals a considerable difference between particle diameters obtained by the two methods for all single annealed materials, which clearly indicates that the particles observed by TEM are actually built up from smaller crystallites. By taking the well-known tendentious particle size overestimation of the Scherrer equation into account, the real crystallite sizes could even be smaller than the calculated values. The second and third sample series exhibited more similar particle diameters when data from calculated and measured datasets were compared (Fig 4b, c), which again confirms the hypothesis that primary crystallites sinter into bigger, denser particles.

3.3 X-ray photoelectron spectroscopy

All functionalized carbon nanotubes were examined by XPS before palladium impregnation in order to determine the amount of their oxygen containing surface functional groups. As data tabulated in Table 3 indicates, non-functionalized nanotubes showed the lowest atomic percent of oxygen, whereas other, acid treated nanotubes possessed significantly higher oxygen amounts. It is important to mention that all functionalized nanotubes featured almost identical amounts of oxygen practically independent of the duration of the functionalization reaction, which suggests that 4 h of oxidation is sufficient to form all possible functional groups on the nanotube surface. The carbonylic to hydroxylic oxygen atom ratios also support this assumption. They are close to one for all samples, which suggests that the oxygen atoms are actually in the form of carboxylic groups. It is on this basis that we hypothesize that the size of the formed palladium nanoparticles is not entirely governed by the raw amount or type of surface functional groups, as particles do become smaller with oxidation time even when XPS no longer indicates any changes in the amount or type of surface functional groups.

3.4 Raman spectroscopy

Raman spectra (depicted in Fig. 3) were measured on all non-impregnated multiwall carbon nanotubes. The main features of the spectra are the two peaks at $\sim$1349 and

Table 3 The ratios of carbonylic to hydroxylic oxygen atoms in all FMWCNT samples as measured by XPS

	C(atomic %)	O(atomic %)	O(carbonyl)/O(hydroxyl)
FMWCNT-0 h	99.17	1.83	0.632
FMWCNT-4 h	88.03	11.97	1.013
FMWCNT-8 h	86.75	13.25	0.996
FMWCNT-12 h	87.57	12.43	1.044
FMWCNT-16 h	86.92	13.08	1.061

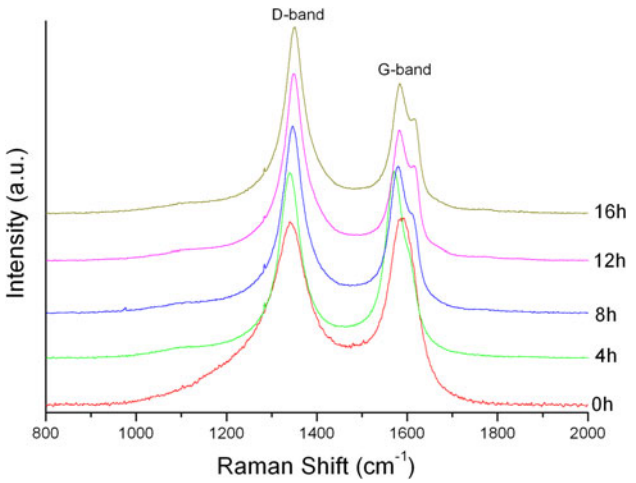

Fig. 3 Raman *D* and *G bands* of all functionalized, non-impregnated multiwall carbon nanotubes

$\sim$1586 cm^{-1} corresponding to the well-known Raman D- and G-bands, respectively. The intensity of the disorder-induced D-band is generally associated with the amount of defects (more precisely, with the amount of sp^3 hybridized phonon scattering sites) in the nanotubes, while the G-band is attributed to the tangential lattice vibrations of sp^2 bonded carbon atoms. As seen in Fig. 4a–c, the G/D band intensity ratios do not change in the first 4 h of functionalization when the primary reaction according to XPS is the oxidation of all available surface sites to –COOH groups. Once all possible carboxyl groups have been formed, subsequent nitric acid treatment results mainly in the increasing of defect site concentration due to e.g. nanotube cutting, amorphous carbon debris formation, nanotube wall

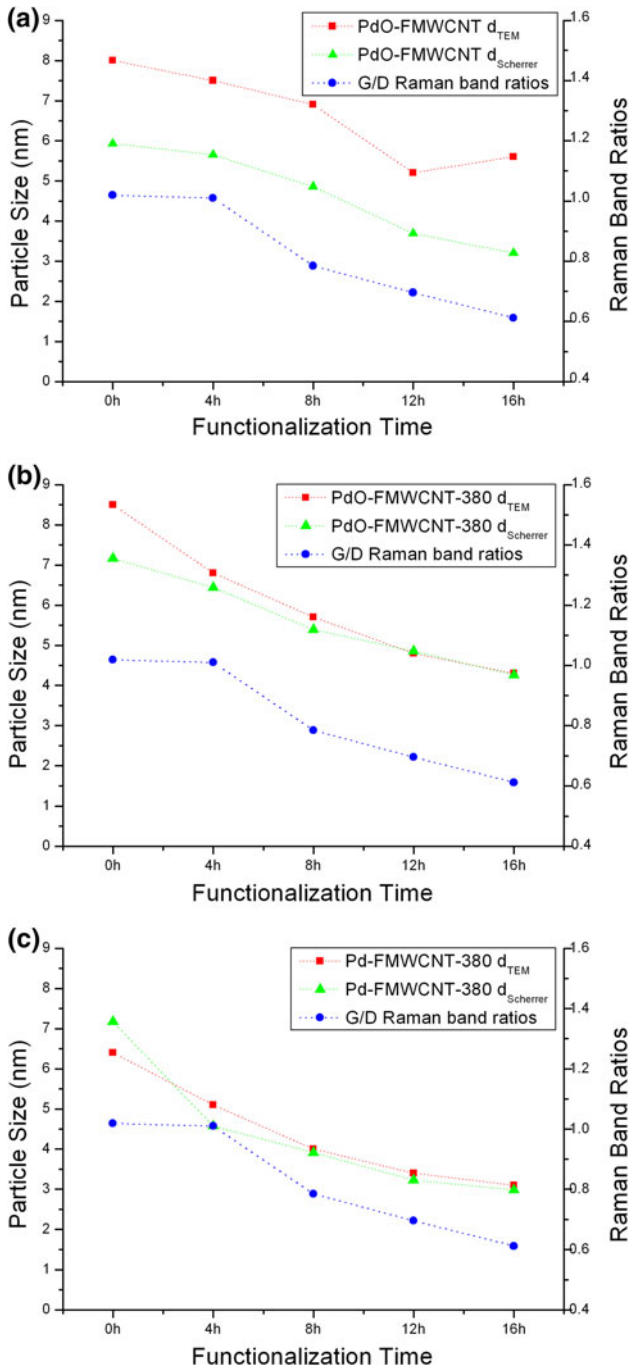

Fig. 4 Comparison of particle diameters obtained by different methods for **a** PdO-FMWCNT, **b** PdO-FMWCNT-380 and **c** Pd-FMWCNT-380 sample series

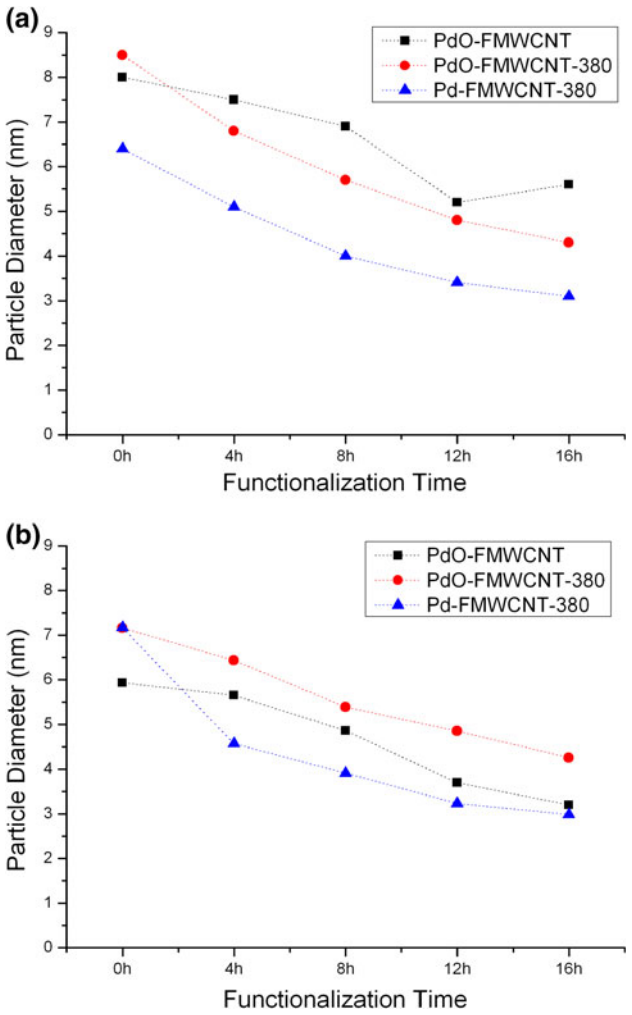

Fig. 5 Comparison of particle diameters obtained by **a** TEM micrograph scaling and **b** calculation with the Scherrer equation

penetration etc. In the later stages of oxidative functionalization there is a direct correlation between the Raman G/D ratio and the nanoparticle size: the smaller the G/D ratio, the smaller the Pd nanoparticles can grow. These suggests that at the onset of nitric acid functionalization the amount of oxygen containing functional groups is the main governing factor behind the sintering and aggregation inhibition of Pd nanoparticles, whereas at functionalization times longer than 4 h the amount of surface defects becomes the major factor. Moreover, previous studies have shown (Li et al. 2012) that oxygen containing functional groups start to decompose at temperatures higher than 130 °C, which suggests that the concentration of functional groups might decrease during preparation and annealing.

4 Conclusion

Multiwalled carbon nanotube supported Pd and Pd-oxide materials were prepared and studied by TEM, XRD, XPS and Raman spectroscopy. In particular, the effect of oxidative carbon nanotube functionalization duration on the size of palladium nanoparticles was investigated. It was found that there is an inverse proportionality correlation between the functionalization time and the diameter of the Pd particles (Fig. 5). Particle size was largely dependent on

the amount of nanotube surface defects, whereas the amount of oxygen containing functional groups appears to have been a critical factor only at the beginning of the nitric acid treatment.

These findings suggest that caution should be exercised when comparing impregnated Pd@MWCNT catalysts even if they were prepared from the same materials and have the same metal loading, as the pretreatment of the nanotube support affects the achievable Pd nanoparticle size systematically. This was exemplified here by the well-known and widespread nitric acid treatment reaction, however, we expect the same general rules to apply to all other functional groups which are formed in any reaction with a potential to modify the amount of nanotube surface defects.

Acknowledgments The financial support of the TÁMOP-4.2.2.A-11/1/KONV-2012-0047 and TÁMOP-4.2.2.A-11/1/KONV-2012-0060 projects is acknowledged. The authors thank Gábor Pótári and Albert Oszkó for the XPS measurements.

References

Antisari, M.V., Marazzi, R., Krsmanovic, R.: Synthesis of multiwall carbon nanotubes by electric arc discharge in liquid environments. Carbon **41**, 2393–2401 (2003)

Antolini, E.: Graphene as a new carbon support for low-temperature fuel cell catalysts. Appl. Catal. **123–124**, 52–68 (2012)

Bayram, E., Zahmakıran, M., Özkar, S., Finke, R.G.: In situ formed "weakly ligated/labile ligand" iridium(0) nanoparticles and aggregates as catalysts for the complete hydrogenation of neat benzene at room temperature and mild pressures. Langmuir **26**, 12455–12464 (2010)

Che, M., Bennett, C.O.: The influence of particle size on the catalytic properties of supported metals. Adv. Catal. **36**, 55–172 (1989)

Corrias, M., Caussat, B., Ayral, A., Durand, J., Kihn, Y., Kalck, Ph, Serp, Ph: Carbon nanotubes produced by fluidized bed catalytic CVD: first approach of the process. Chem. Eng. Sci. **58**, 4475–4482 (2003)

Dalai, A.K., Davis, B.H.: Fischer–Tropsch synthesis: a review of water effects on the performances of unsupported and supported Co catalysts. Appl. Catal. **348**, 1–15 (2008)

Dikonimos Makrisa, Th, Giorgi, R., Lisi, N., Pilloni, L., Salernitano, E., Sarto, F., Alvisi, M.: Carbon nanotubes growth by HFCVD: effect of the process parameters and catalyst preparation. Diam. Relat. Mater. **13**, 305–310 (2004)

Gallagher, P.K., Gross, M.E.: The thermal decomposition of palladium acetate. J. Therm. Anal. **31**, 1231–1241 (1986)

Gates, B.C.: Supported metal clusters: synthesis, structure, and catalysis. Chem. Rev. **95**, 511–522 (1995)

Georgakilas, V., Gournis, D., Tzitzios, V., Pasquato, L., Guldi, D.M., Prato, M.: Decorating carbon nanotubes with metal or semiconductor nanoparticles. J. Mater. Chem. **17**, 2679–2694 (2007)

Geus, J.W., van Dillen, A.J.: In: Ertl, G., Knözinger, H., Weitkamp, J. (eds.) Preparation of Solid Catalysts, vol. 6, pp. 460–487. Wiley, Weinheim (1999)

Halonen, N., Rautio, A., Leino, A.R., Kyllonen, T., Toth, G., Lappalainen, J., Kordas, K., Huhhtanen, M., Keiski, R.L., Sapi, A., Szabo, M., Kukovecz, A., Konya, Z., Kiricsi, I., Ayajan, P.M., Vajtai, R.: Three-dimensional carbon nanotube scaffolds as particulate filters and catalyst support membranes. ACS Nano **4**, 2003–2008 (2010)

Height, M.J., Howard, J.B., Tester, J.W., Sande Vander, J.B.: Flame synthesis of single-walled carbon nanotubes. Carbon **42**, 2295–2307 (2004)

Hernadi, K., Konya, Z., Siska, A., Kiss, J., Oszkó, A., Nagy, J.B., Kiricsi, I.: On the role of catalyst, catalyst support and their interaction in synthesis of carbon nanotubes by CCVD. Mater. Chem. Phys. **77**, 536–541 (2003)

Horvath, E., Puskas, R., Remias, R., Mohl, M., Kukovecz, A., Konya, Z., Kiricsi, I.: A novel catalyst type containing noble metal nanoparticles supported on mesoporous carbon: synthesis. Charact. Catal. Prop. Top. Catal. **52**, 1242–1250 (2009)

Komiyama, M.: Design and preparation of impregnated catalysts. Catal. Rev. Sci. Eng. **27**, 341–372 (1985)

Konya, Z., Vesselenyi, I., Niesz, K., Kukovecz, A., Demortier, A., Fonseca, A., Delhalle, J., Mekhalif, Z., Nagy, B.J., Koos, A.A., Osvath, Z., Kocsonya, A., Biro, L.P., Kiricsi, I.: Large scale production of short functionalized carbon nanotubes. Chem. Phys. Lett. **360**, 429–435 (2002)

Kukovecz, A., Konya, Z., Nagaraju, N., Willems, I., Tamasi, A., Fonseca, A., Nagy, J.B., Kiricsi, I.: Catalytic synthesis of carbon nanotubes over Co, Fe and Ni containing conventional and sol–gel silica–aluminas. Phys. Chem. Chem. Phys. **2**, 3071–3076 (2000)

Lebedkin, S., Schweiss, P., Renker, B., Malik, S., Hennrich, F., Neumaier, M., Stoermer, C., Kappes, M.: Single-wall carbon nanotubes with diameters approaching 6 nm obtained by laser vaporization. Carbon **40**, 417–423 (2002)

Li, C., Shao, Z., Pang, M., Williams, C.T., Liang, C.: Carbon nanotubes supported Pt catalysts for phenylacetylene hydrogenation: effects of oxygen containing surface groups on Pt dispersion and catalytic performance. Catal. Today **186**, 69–75 (2012)

Liu, H.P., Cheng, G., Zheng, R.T., Zhao, Y., Liang, C.L.: Influence of acid treatments of carbon nanotube precursors on Ni/CNT in the synthesis of carbon nanotubes. J. Mol. Catal. **230**, 17–22 (2005)

Park, D., Kim, J.H., Lee, J.K.: Synthesis of carbon nanotubes on metallic substrates by a sequential combination of PECVD and thermal CVD. Carbon **41**, 1025–1029 (2003)

Puskas, R., Sapi, A., Kukovecz, A., Konya, Z.: Comparison of nanoscaled palladium catalysts supported on various carbon allotropes. Top. Catal. **55**, 865–872 (2012)

Sachtler, W.M.H.: In: Ertl, G., Knözinger, H., Weitkamp, J. (eds.) Handbook of Heterogeneous Catalysis, vol. 1, pp. 365–374. Wiley, Weinheim (1997)

Sapi, A., Remias, R., Konya, Z., Kukovecz, A., Kordas, K., Kiricsi, I.: Synthesis and characterization of nickel catalysts supported on different carbon materials. React. Kin. Catal. Lett. **96**, 379–389 (2009)

Seelam, P.K., Huuhtanen, M., Sapi, A., Szabo, M., Kordas, K., Turpeinen, E., Toth, G., Keiski, R.L.: CNT-based catalysts for H_2 production by ethanol reforming. Int. J. Hydrogen Energy **35**, 12588–12595 (2010)

Serp, P., Corrias, M., Kalck, P.: Carbon nanotubes and nanofibers in catalysis. Appl. Catal. **253**, 337–358 (2003)

Silva, W.M., Ribeiro, H., Seara, L.M., Calado, H.D.R., Ferlauto, A.S., Paniago, R.M., Leite, C.F., Silva, G.G.: Surface properties of oxidized and aminated multi-walled carbon nanotubes. J. Braz. Chem. Soc. **23**, 1078 (2012)

Tang, S.H., Sun, G.Q., Sun, S.G., Qi, J., Xin, Q., Haarberg, G.M.: Double-walled carbon nanotubes as catalyst support in direct methanol fuel cells. J. Electrochem. Soc. **157**, B1321–B1325 (2010)

Vermisoglou, E.C., Romanos, G.E., Karanikolos, G.N., Kanellopoulos, N.K.: Catalytic NOx removal by single-wall carbon nanotube-supported Rh nanoparticles. J. Hazard Mater. **194**, 144–155 (2011)

Wu, H.M., Wexler, D., Wang, G.X., Liu, H.K.: Pt/C catalysts using different carbon supports for the cathode of PEM fuel cells. Adv. Sci. Lett. **4**, 115–120 (2011)

Wu, J., Xue, Y., Yan, X., Yan, W.S., Cheng, Q.M., Xie, Y.: Co_3O_4 nanocrystals on single-walled carbon nanotubes as a highly efficient oxygen-evolving catalyst. Nano Res. **5**, 521–530 (2012)

Xiong, H.F., Motchelaho, M.A.M., Moyo, M., Jewell, L.L., Coville, N.J.: Correlating the preparation and performance of cobalt catalysts supported on carbon nanotubes and carbon spheres in the Fischer-Tropsch synthesis. J. Catal. **278**, 26–40 (2011)

Yabe, Y., Ohtake, Y., Ishitobi, T., Show, Y., Izumi, T., Yamauchi, H.: Synthesis of well-aligned carbon nanotubes by radio frequency plasma enhanced CVD method. Diam. Relat. Mater. **13**, 1292–1295 (2004)

Zhang, Y.: Synthesis of few-walled carbon nanotube–Rh nanoparticles by arc discharge: effect of selective oxidation. Mater. Charact. **68**, 102–109 (2012)